RSC Advances

PAPER

View Article Online
View Journal | View Issue

Cite this: *RSC Adv.*, 2014, **4**, 18222

A high-performance polyurethane sponge for the detection, adsorption and separation of Cu^{2+} ions

Yun Yu,[a] Jianrui Wang,[a] Jiansheng Lian[b] and Xinjian Cheng*[a]

Received 7th March 2014
Accepted 26th March 2014

DOI: 10.1039/c4ra01981d

www.rsc.org/advances

The simultaneous detection and separation of copper ions is important. In this study, a fluorescent chemosensor (a copper sensitive molecule), was prepared using 6-bromo-benzo[*de*]isochromene-1,3-dione as a precursor. The as-prepared fluorescent molecule contains a hydroxyl group and an aminoquinoline moiety. The hydroxyl group enables the fluorescent molecule to anchor to a porous polyurethane (PU) sponge. The chemosensors still retained their recognition ability after they were introduced to PU. Upon the addition of Cu^{2+} ions to the PU sponge, both the color and the fluorescence intensity changed, suggesting that the chemosensor-functionalized PU sponges could be used as a Cu^{2+} ion sensor. The copper ions could also accumulate and be enriched on the sponges. The adsorption capacity of the PU sponge (containing 2 wt% of the chemosensor) reached 97.26 mg g^{-1}, which was higher than that of the solid PU membranes (52.62 mg g^{-1}). These polymeric, highly sensitive chemosensors may potentially be applied in the detection of water pollution generated by sources such as electroplating and drain outflow.

1. Introduction

The pollution caused by heavy metal ions, especially in aqueous systems, is one of the most dangerous and serious environmental problems owing to the bioaccumulation of these toxic metal ions.[1,2] Copper plays a vital role in various biological processes[3] and is a micronutrient essential to human health.[4] However, copper causes oxidative stress and might be harmful to liver and kidney function[5] at high concentrations. Hence, the upper limit of copper in drinking water is established at 1.3 ppm by the U.S. Environmental Protection Agency, and the concentration of copper in blood is limited to 100–150 μg dL^{-1} (15.7–23.6 μM).[6] Therefore, a rapid and convenient method for detecting copper is of importance due to water quality[7,8] and biological concerns.[9,10]

In many works, traditional methods of detecting copper involved synthesizing small molecular chemosensors. For example, Yang *et al.*[11] reported three new rhodamine Schiff base sensors. They provided Cu^{2+} selectivity and sensitivity through the rhodamine ring-open approach and demonstrated the fluorescent imaging of Cu^{2+} in living cells. Lee *et al.*[12] reported novel rhodamine hydrazone derivatives containing an additional phenol group that showed a high selectivity for Cu^{2+} and reversible colorimetric change with Cu^{2+}. Yu *et al.*[13] reported a fluorescent chemodosimeter based on the 1,8-naphthyridyl moiety. This chemodosimeter displayed highly selective behavior for Cu^{2+}. Jung *et al.*[14] developed a novel coumarin-based fluorescent chemosensor that showed a high selectivity for Cu^{2+} and a suitable affinity for Cu^{2+} in biologic functions. They also employed the chemosensor for the fluorescent detection of intracellular Cu^{2+} in cells. However, many of these chemosensors only have a high sensitivity and selectivity for detecting Cu^{2+};[15–17] they cannot separate Cu^{2+} from the solution because the chemosensors are soluble or dispersible in water. Even after combining with Cu^{2+}, they still remain in the water.

To overcome this drawback, a novel method was created that immobilized the chemosensor on macromolecules. This strategy not only retained the chemosensor sensitivity, but also improved its operability and convenience for the separation of heavy metals.

In this work, a new chemosensor was synthesized and introduced to porous PU sponge. The chemosensor-functionalized PU sponge (FPU) could selectively detect and separate Cu^{2+} ions. The small molecule was first synthesized by the reaction of 6-bromo-benzo[*de*]isochromene-1,3-dione with ethanolamine and 8-aminoquinoline, introducing the quinoline and hydroxyl groups. The FPU sponge was then formed *via* reaction of the hydroxyl groups on the chemosensor and the isocyanate groups of 2,4-tolylene diisocyanate (TDI). The PU was foamed by adding a suitable amount of water and then heated and aged to obtain the porous FPU sponge. This FPU sponge showed excellent detecting and separating ability for Cu^{2+} concentrations as low as 10^{-7} mol L^{-1}. It is better than functional solid membranes due to the higher specific surface area. The functional sponge has potential applications in the detection and separation of Cu^{2+} pollutants.

---

[a] School of Chemistry and Materials Science, South-Central University for Nationalities, Wuhan, 430074, China. E-mail: chxj606@163.com

[b] LMB, South China Sea Institute of Oceanology, Chinese Academy of Sciences, Guangzhou, 510301, China

2. Experimental section

2.1 Materials

A precursor for the fluorescent co-monomer, 6-bromo-benzo[*de*]-isochromene-1,3-dione, was purchased from J&K China Chemical Ltd. and recrystallized twice with chlorobenzene. Ethanolamine, 8-aminoquinoline and tri(dibenzylideneacetone) dipalladium(0) ($Pd_2(dba)_3$) were bought from J&K China Chemical Ltd. (+/−)-2,2′-Bis(diphenylphosphino)-1,1′-binaphthyl (BINAP) and sodium tertiary butoxide were products of Aladdin Chemical Co., Ltd.

All metal salts (Cr^{3+}, Co^{2+}, Pd^{2+}, Zn^{2+}, Hg^{2+}, Mn^{2+}, Ni^{2+}, Pb^{2+}, Cu^{2+}, Fe^{2+} and Fe^{3+}) were purchased from Aladdin Chemical Co., Ltd. and used as received.

2,4-Tolylene diisocyanate (TDI) and poly(oxyethylene) (PEG 600) with a molecular weight of 600 were from Aladdin Chemical Co., Ltd, and dibutyltin dilaurate, triethanolamine, absolute ethanol, toluene and tetrahydrofuran (THF) were purchased from J&K China Chemical Ltd. Ultrapure water (>17 MΩ cm^{-1}) from a Milli-Q water system was used throughout the experiments.

2.2 Preparation of 6-bromo-2-(2-hydroxy-ethyl)-benzo[*de*]-isoquinoline-1,3-dione (BHD)

BHD was prepared by a modified method according to the literature[21] using the following procedure: 6-bromo-benzo[*de*]-isochromene-1,3-dione (0.2 g, 0.7 mmol) was reacted with ethanolamine (0.06 mL, 0.7 mmol) by refluxing for 4 h in 35 mL of absolute ethanol. After cooling to room temperature, the suspension solution was filtered and washed with ethanol. The crude compound was further purified by recrystallization form ethanol and dried to give the pale yellow product BHD (0.21 g) with a 90% yield.

2.3 Synthesis of 2-(2-hydroxy-ethyl)-6-(quinolin-8-ylamino)-benzo[*de*]isoquinoline-1,3-dione (HQD)

A dried round-bottom flask was charged with BHD (0.1 g, 0.3 mmol), 8-aminoquinoline (0.086 g, 0.6 mmol), BINAP (7 mg), $Pd_2(dba)_3$ (5 mg), and sodium tertiary butoxide (120 mg). Toluene (50 mL) was added and the solution was degassed under a nitrogen atmosphere, stirred for 1 h in an ice bath, and heated to 90 °C for 48 h. The reaction mixture was cooled and filtered through a Celite pad and washed with dichloromethane. The residue concentrated *in vacuo* was purified by flash column chromatography (ethyl acetate–hexane = 4 : 1) to give HQD (57 mg, 48% yield).

2.4 Synthesis of chemosensor functionalized PU sponge (FPU sponge)

The porous FPU sponges were prepared by the condensation reaction of TDI isocyanate groups with PEG hydroxyl groups at a ratio of 1.5 : 1. Different amounts of HQD were added at room temperature. The catalysts dibutyltin dilaurate (1 wt%) and triethanolamine (1 wt%) were added after stirring for 10 minutes. Finally, water (0.1 mL) was added as a foaming agent. The FPU sponge was obtained after heating at 60 °C and aging. The chemosensor, HQD, was added at different weight percentages (0.5, 1, 1.5, and 2 wt%), and the obtained samples were extracted with ethanol to wash and remove the residual small molecules and catalysts.

2.5 Synthesis of solid FPU membranes

The process of preparing solid PU membranes was as follows: different amounts of HQD (0.5, 1, 1.5, and 2 wt%) and THF (30 mL) were added to 1.5 : 1 ratios of TDI to PEG. After stirring for 2 h at 60 °C, the solution was poured onto a glass slide and dried at room temperature, yielding the solid PU membranes.

2.6 Characterization

FTIR and ^{1}H NMR measurements. Fourier transform infrared spectra (FTIR, 4000–500 cm^{-1}) were collected on a Nicolet NEXUS 470 spectrometer. The samples were pressed into KBr pellets for measurements. Nuclear magnetic resonance (^{1}H NMR) was measured in DMSO on an AVANCE III-400 (Bruker) spectrometer.

Fluorescence measurements and fluorescence imaging. Fluorescence spectra were collected on a Perkin Elmer lambda 35 spectrometer using an excitation wavelength of 446 nm. Fluorescence images were photographed with a Bx61 fluorescence microscope.

UV-Vis experiments. Solid and liquid samples were analyzed with a Perkin Elmer lambda 35 UV-Vis spectrometer.

Atomic absorption spectrometry (AAS). Metal ion solutions were prepared in water while HQD solutions were prepared in DMF. Copper concentrations (below 10 mg L^{-1}) were determined by an AA-6300 atomic absorption spectrometer.

X-ray photoelectron spectroscopy (XPS) measurements. XPS analysis was carried out with a Thermo VG Multilab 2000 spectrometer using an Al Kα X-ray source (300 W PE 25 eV).

3. Results and discussion

3.1 Synthesis and characterization of chemosensor HQD

HQD was prepared using the procedure shown in Scheme 1(a). Based on the property of 4-bromo-naphthalic anhydride, the amidation reaction of the anhydride was conducted moderately easily. The desired small molecule was synthesized by a Pd-catalyzed (BINAP, $Pd_2(dba)_3$ and sodium tertiary butoxide) aryl amination between 6-bromo-2-(2-hydroxy-ethyl)-benzo[*de*]isoquinoline-1,3-dione and 8-aminoquinoline. The chemosensor HQD was obtained in 48% yield after purification by flash column chromatography. Fig. 1 shows the FT-IR spectra of the small molecule (HQD) and the starting material. The strong C–O–C peaks at 1778 cm^{-1} and 1733 cm^{-1} disappeared and new peaks at 1698 cm^{-1} and 1663 cm^{-1} were determined by comparison with the peaks of 6-bromo-benzo[*de*]isochromene-1,3-dione. The C–Br peak at 556 cm^{-1} disappeared and a new C–N peak of 1366 cm^{-1} emerged. This means that the Pd-catalyzed aryl amination reaction between 6-bromo-2-(2-hydroxy-ethyl)-benzo[*de*]isoquinoline-1,3-dione and 8-aminoquinoline was successful.

To further verify the structure of HQD, the ^{1}H NMR spectrum is shown in Fig. 2. It can be seen that the peaks ranging from 8.2

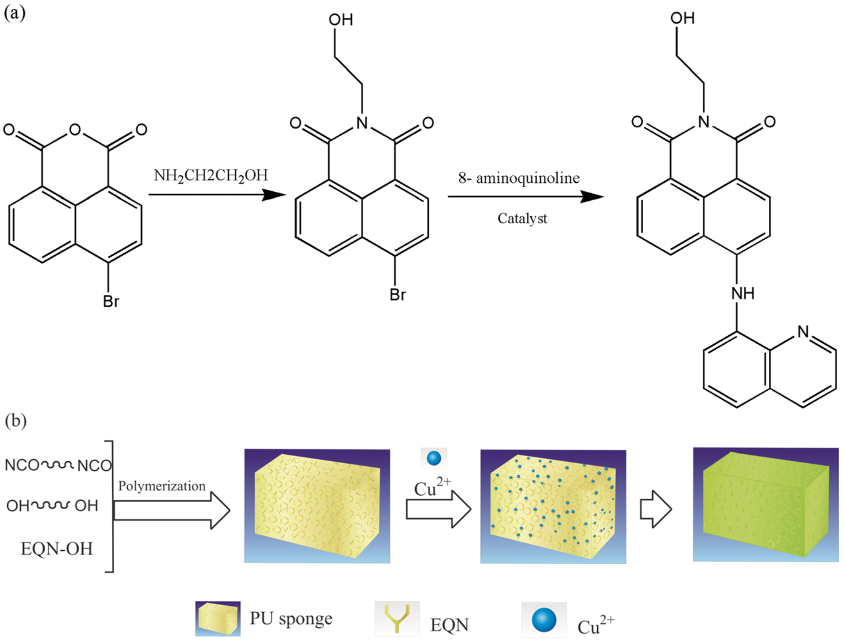

Scheme 1 (a) The synthetic route of chemosensor HQD and (b) preparation of the FPU sponge.

to 8.7 ppm represent the H in the naphthalene ring, and the peaks at about 4.3 ppm and 3.8 ppm represent the two $-CH_2-$ groups (the red line in Fig. 2). Compared to the spectrum of BHD, that of HQD (the lower line in Fig. 2) portrays that the new quinoline peaks appeared between 6.7 ppm and 7.3 ppm and at 5.8 ppm. Moreover, the naphthalene ring H peaks are reduced by about 0.3 ppm owing to the introduction of the quinoline ring.

3.2 Synthesis and characterization of polyurethane sponges

TDI and PEG are usually used to prepare polyurethane films and foams.[18–20] The process for the preparation of the FPU sponge is shown in Scheme 1(b). The FPU sponge was synthesized with a simple and quick method that used water as the foaming agent under catalysis without solvent. Fig. 3 shows the XPS scans of PU membrane and the PU sponge upon adsorption of Cu^{2+}. In order to confirm the polymerization of the TDI isocyanate groups with the BHD hydroxyl groups, Br was analyzed after the polymerization reaction of TDI, PEG and BHD. As shown in Fig. 3a and b, the small molecules were successfully polymerized onto polyurethane. When the FPU sponge was analyzed by XPS, the N peaks could not be easily distinguished because both HDQ and PU contain N atoms. The BHD-containing PU was analyzed to confirm that sensitive molecules could be introduced to PU using this method. The FPU sponge containing Cu^{2+} (indicated by a color change from yellow to green) was extracted, rinsed and evaporated. Subsequent analysis by XPS indicated the presence of Cu atoms (Fig. 3c and d), further confirming the formation of the Cu–PU sponge.

The fluorescence imaging (Fig. 4) further confirmed that the chemosensor was introduced into the PU sponge and displayed

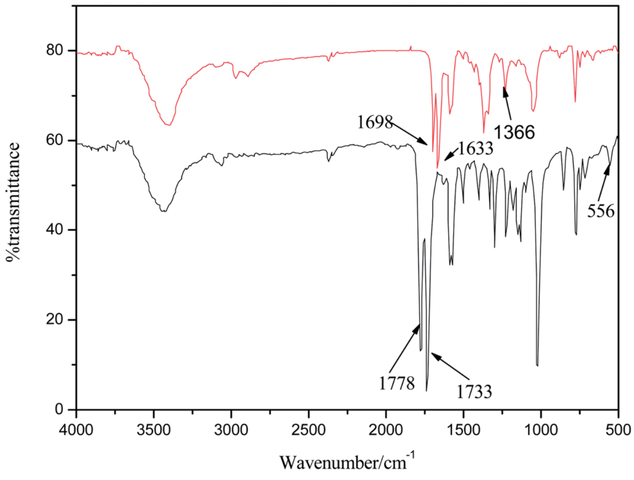

Fig. 1 The FT-IR spectrum of the starting material (black line) and the chemosensor (HQD) (red line).

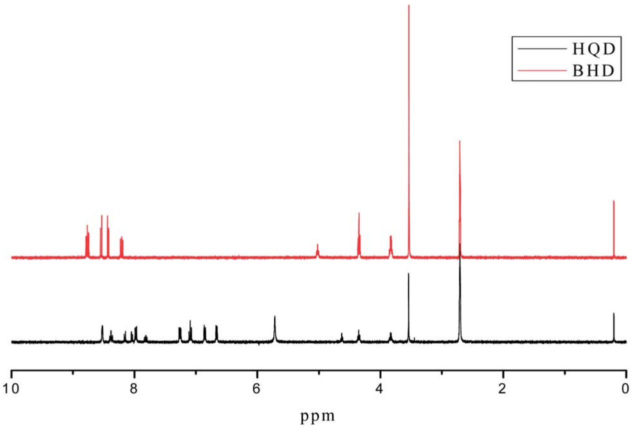

Fig. 2 The ^1H NMR spectrum of BHD (red line) and the chemosensor HQD (black line).

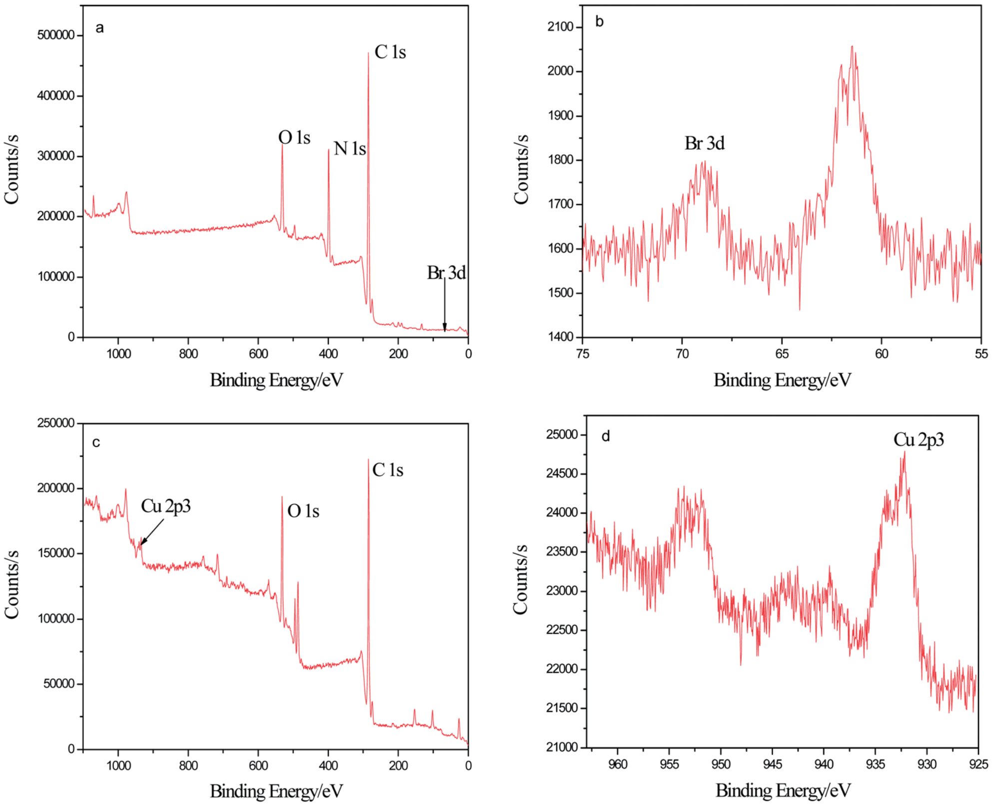

Fig. 3 XPS spectra of (a) PU membrane containing small molecule BHD, (b) Br on the PU membrane, (c) adsorption Cu^{2+} of the FPU sponge, and (d) Cu^{2+} on the FPU sponge.

fluorescence without Cu^{2+} ions. The fluorescence was enhanced upon the addition of copper ions.

3.3 Detection of Cu^{2+} by PU sponges

As shown in Fig. 5a, the PU sponges bearing 1.0 wt% HQD were cut into pieces (1 cm × 1 cm × 1 cm) and soaked in solutions containing different concentrations of Cu^{2+} (10^{-2} mol L^{-1}, 10^{-3} mol L^{-1}, 10^{-4} mol L^{-1}, 5×10^{-5} mol L^{-1}, 10^{-5} mol L^{-1}, 10^{-6} mol L^{-1}, and 0 mol L^{-1}). The color of the PU sponges changed obviously from yellow to green (Fig. 5b and c). In order to avoid overlap in color between the yellow sponge and the blue Cu^{2+} ions, some control experiments were also performed. Under the same conditions, PU sponges were placed into blue ink and a solution of Cd^{2+}. It can be seen that the color (yellow) of the PU sponges did not undergo any changes. When pure PU sponges (containing no chemosensor) were treated in this way, they were observed to have no adsorption affinity for Cu^{2+} ions. These results indicated that the color change was only caused by the interaction between HQD and Cu^{2+} ions. The color change could be seen by the naked eye even at Cu^{2+} ion concentrations as low as 5×10^{-5} mol L^{-1}.

The optical properties of the PU sponge determined by UV-Vis spectroscopy are displayed in Fig. 6. The introduction of the chemosensor obviously enhanced the absorbance of the FPU sponge between 500 nm and 800 nm, and the new absorbance at about 680 nm appeared and increased with the concentration of Cu^{2+}.

Fluorescence intensity of the PU sponge both with and without Cu^{2+} ions was measured. Fig. 7a shows the fluorescence of HQD; it increased significantly with increasing Cu^{2+} concentrations at about 516 nm (excited at 446 nm). The Stokes

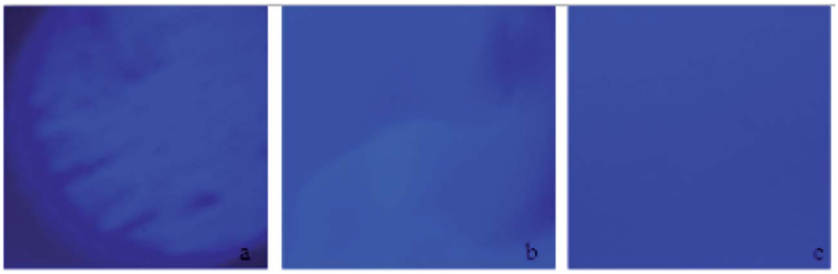

Fig. 4 Fluorescence imaging of (a) the FPU sponge, (b) the FPU sponge with Cu^{2+} ions, and (c) the solid FPU membranes with Cu^{2+} ions.

Fig. 5 (a) Photographs of the color changes in FPU sponges with different concentrations of Cu^{2+} (10^{-2} mol L^{-1}, 10^{-3} mol L^{-1}, 10^{-4} mol L^{-1}, 5×10^{-5} mol L^{-1}, 10^{-5} mol L^{-1}, 10^{-6} mol L^{-1} and 0 mol L^{-1}, from left to right), (b) photographs of the color change in the dry FPU sponge without Cu^{2+} and (c) the dry FPU sponge with Cu^{2+}.

shift is at about 70 nm. Fig. 7b shows that the fluorescence of PU sponges bearing HQD has the same trend as in HQD. This means that the performance of the chemosensor still remains when co-polymerised into the PU sponges. Furthermore, the concentration of Cu^{2+} ions could be detected by the fluorescence intensity in concentrations as low as 10^{-7} mol L^{-1}.

In addition to Cu^{2+}, the possibility of other heavy metal ions interfering with the fluorescence intensity of FPU sponges was investigated (Fig. 8). The fluorescence intensities of FPU sponges were clearly enhanced by Cu^{2+} ions while there was no obvious response to other heavy metal ions (Ni^{2+}, Co^{2+}, Cr^{2+}, Fe^{2+}, Fe^{3+}, Hg^{2+}, Zn^{2+}, Mn^{2+}, Cd^{2+}, and Pb^{2+}; Fig. 8a). The control experiments (Fig. 8b) were performed in the presence of 10^{-4} mol L^{-1} Cu^{2+} mixed with 10^{-4} mol L^{-1} of other heavy metal ions, such as Ni^{2+}/Cu^{2+}, Co^{2+}/Cu^{2+}, Fe^{2+}/Cu^{2+}, Fe^{3+}/Cu^{2+}, Cr^{2+}/Cu^{2+}, Hg^{2+}/Cu^{2+}, Zn^{2+}/Cu^{2+}, Mn^{2+}/Cu^{2+}, Cd^{2+}/Cu^{2+}, and Pb^{2+}/Cu^{2+}. As shown in Fig. 8, Cu^{2+} was the only detected species and no other metal ions interfered with the fluorescence intensity. By measuring I_F/I_0 at 516 nm (I_0 represents the emission intensity of the PU sponge without Cu^{2+} and I_F corresponds to the fluorescence intensity), it could be seen (Fig. 8b) that I_F/I_0 had not been influenced by other common wastewater ions in the binary mixture of copper and other metal ions. The values of I_F/I_0 remained almost the same. The results further indicated that the FPU sponge had a high selectivity for Cu^{2+}.

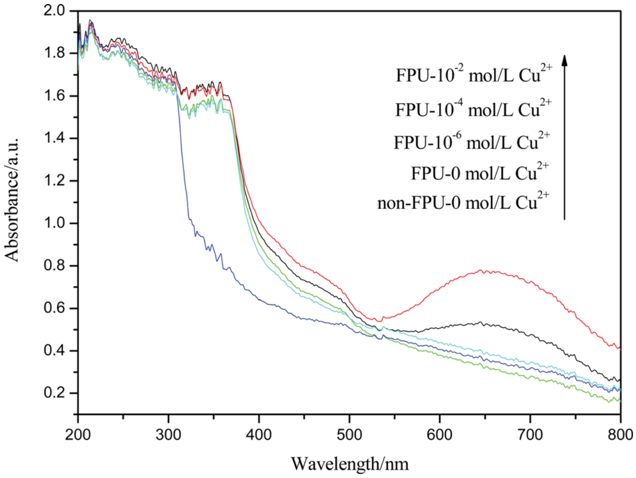

Fig. 6 UV-Vis spectra of the dry FPU sponge and non-FPU sponge (the non-functionalized PU sponge, blue line).

3.4 The effect of pH on Cu^{2+} adsorption by the FPU sponge

The effect of pH on the FPU sponge was evaluated by testing various pH values (2–12) on the adsorption of Cu^{2+} ions (3 mL, 7 mg L^{-1}) by the FPU sponge. As shown in Fig. 9, the adsorption capacity of the FPU sponge remained almost constant at pH values from 4–10. At pH values below 4.0 and above 10, the adsorption capacity decreased. Below pH 4, the protonation of N atoms occurred, reducing the sponge's ability to complex copper ions. In strong alkaline conditions (pH ≥ 12), the adsorption capacity of the FPU sponge also decreased. This might be attributed to the following two reasons: (1) at high pH, $Cu(OH)_2$ formed, decreasing the number of copper ions coordinated to the chemosensors and (2) the porous PU sponges collapsed at high pH, resulting in a reduction of specific surface area and a decrease in adsorption ability. These results suggest that this PU sponge could have a high copper ion adsorption ability in the pH range of 4–10.

3.5 Dynamic adsorption capacity of the FPU sponge

Dynamic adsorption capacity with Cu^{2+} ions was measured. The as-prepared PU sponge was fixed in the middle of two PMMA columns (Fig. 10). A series of same-volume solutions (100 mL) containing different concentrations of Cu^{2+} (10^{-6} mol L^{-1}, 10^{-5} mol L^{-1}, and 10^{-4} mol L^{-1}) were poured into the PMMA column and passed through the PU sponge. The elapsed time and solution volume were recorded. The equilibrium concentrations in the solutions passing through the PU sponge were quantified by AAS. The adsorption capacity of Cu^{2+} on the PU sponge was calculated by the following equation,

$$q = \frac{(C_0 - C_e) \times V}{W} \tag{1}$$

where q represents the absorptivity capacity (%), C_0 and C_e represent the concentration of Cu^{2+} ions before the adsorption experiment and the equilibrium concentration of Cu^{2+} in mg L^{-1}, respectively. V is the volume of the Cu^{2+} solution and W is the weight of the PU sponge.

Equilibrium concentrations of the solutions passing through the FPU sponge are listed in Table 1. Under the same continuous flow and time conditions, the adsorption capacity was significantly enhanced with increasing Cu^{2+} concentration.

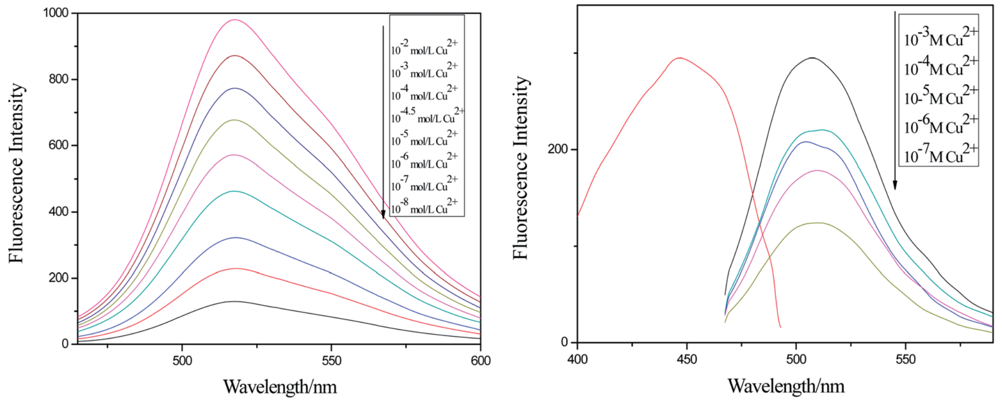

a b

Fig. 7 Fluorescence spectra of the chemosensor (a) and the dry FPU sponge (b).

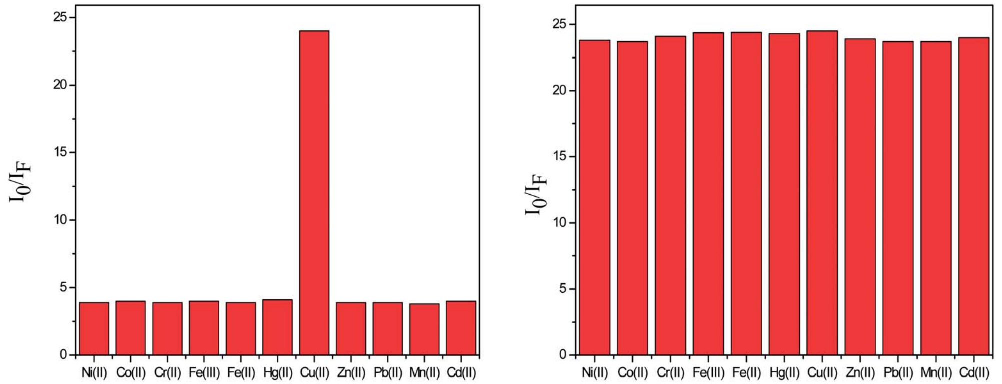

(a) (b)

Fig. 8 The florescence response of the FPU sponge containing 1 wt% HQD to metal ions for (a) the single metal ions (10^{-4} mol L^{-1}) and (b) the mixture of Cu^{2+}(10^{-4} mol L^{-1}) and other metal ions (Ni^{2+}, Co^{2+}, Cr^{2+}, Fe^{2+}, Fe^{3+}, Hg^{2+}, Zn^{2+}, Mn^{2+}, Cd^{2+}, and Pb^{2+}; 10^{-4} mol L^{-1}).

In addition, static adsorption capacity was measured using an FPU sponge and a solid FPU membrane. They were put into Cu^{2+} solutions with the same volume and concentration and

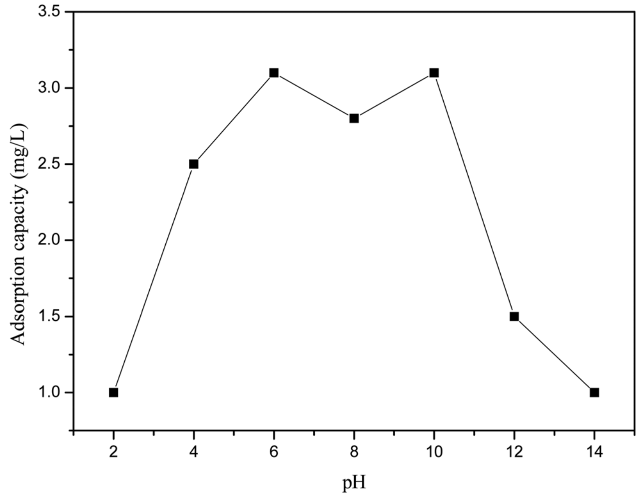

Fig. 9 The adsorption capacity of the FPU sponge for Cu^{2+} ions (3 mL, 7 mg L^{-1}) at varying pH (2–12).

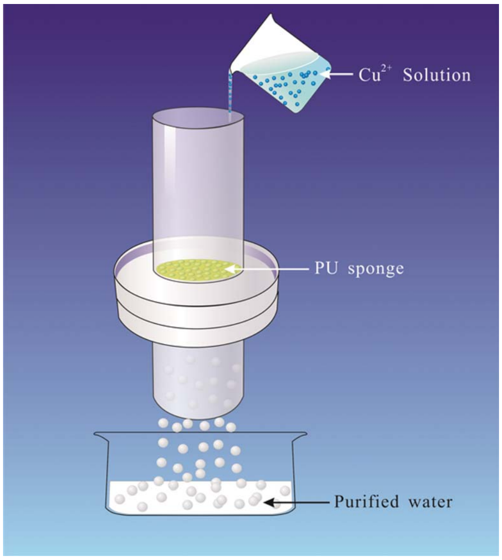

Fig. 10 Schematic diagram of the dynamic adsorption procedure of Cu^{2+} ions from solution using the fabricated FPU sponge as a filter.

Table 1 Dynamic adsorption capacity per unit content and unit time of the FPU sponge

Concentration of Cu^{2+} ions, C_0 (mg L^{-1})	0.1596	1.596	7.88	15.96
Concentration of Cu^{2+} ions, C_e (mg L^{-1})	0.025	0.6280	6.215	14.275
Volume of Cu^{2+} ions V (mL)	100	100	100	100
Adsorption capacity per unit time (mg g^{-1})	8.87	53.77	92.48	93.57

Table 2 Static adsorption capacity per unit content and unit time of the FPU sponge and the solid FPU membrane

HQD content (1 wt%)	0.5	1.0	1.5	2.0	Solid membrane 2.0
Concentration of Cu^{2+} C_0 (mg L^{-1})	5	5	5	5	5
Concentration of Cu^{2+} C_e (mg L^{-1})	4.1693	3.7572	3.3967	3.2494	4.0528
Volume of the Cu^{2+} solution V (mL)	100	100	100	100	100
Adsorption capacity per unit time (mg g^{-1})	46.15	69.04	89.07	97.26	52.62

then removed at the same time. The Cu^{2+} concentrations before and after removal were measured and listed in Table 2. It could be seen that the content of HQD dramatically affected the adsorption capacity of the FPU sponge. Higher HQD content was associated with higher adsorption capacity per unit time. However, the solid FPU membrane was inferior for Cu^{2+} adsorption compared to the FPU sponge. It may be attributed to the high specific surface area of the FPU sponge which provided more opportunities and spaces to complex and remove Cu^{2+} ions. These results suggest that the FPU sponge could be used for filtration or purification of Cu^{2+}-containing solutions.

4. Conclusion

In conclusion, a fluorescent monomer, 2-(2-hydroxy-ethyl)-6-(quinolin-8-ylamino)-benzo[*de*]isoquinoline-1,3-dione (HQD) was synthesized and introduced to a solid FPU membrane and a porous FPU sponge to form a macromolecular chemosensor for Cu^{2+} ions. After the chemosensor was co-polymerised onto the surfaces of the PU sponge, it still retained fluorescence performance. Compared to the PU solid membrane, the FPU sponge had the advantages of greater specific surface area and adsorption capacity. Furthermore, the as-prepared FPU sponge can not only detect but also remove and recycle Cu^{2+} ions without any complicated post-processing.

Acknowledgements

The authors would like to thank the financial support of National Natural Scientific Foundation of China (NSFC 41240026) and Guangdong Natural Science Foundation (S201210009845).

References

1 K. Zargoosh, H. Abedini, A. Abdolmaleki and M. R. Molavian, *Ind. Eng. Chem. Res.*, 2013, **52**, 14944.
2 Y. A. Hu and H. F. Cheng, *Environ. Sci. Technol.*, 2013, **47**, 3752.
3 L. S. Sarma, J. R. Kumar, K. J. Reddy and A. V. Reddy, *J. Agric. Food Chem.*, 2005, **53**, 5492–5498.
4 M. A. Tarighat, M. R. Mohammadizadeh and G. Abdi, *J. Agric. Food Chem.*, 2013, **61**, 6832.
5 X. M. Wu, Z. Q. Guo, Y. Z. Wu, S. Q. Zhu, T. D. James and W. H. Zhu, *ACS Appl. Mater. Interfaces*, 2013, **5**, 12215.
6 H. D. Song, I. Choi, S. Lee, Y. I. Yang, T. Kang and J. Yi, *Anal. Chem.*, 2013, **85**, 7980.
7 Z. L. Gong and Y. W. Zhong, *Organometallics*, 2013, **32**, 7495.
8 H. Bessbousse, J. F. Verchère and L. Lebrun, *Chem. Eng. J.*, 2012, **187**, 16.
9 S. L. Hu, Q. Zhao, Y. Dong, J. L. Yang, J. Liu and Q. Chang, *Langmuir*, 2013, **29**, 12615–12621.
10 M. H. Lee, J. H. Han, J. H. Lee, N. Park, R. Kumar, C. Kang and J. S. Kim, *Angew. Chem., Int. Ed.*, 2013, **52**, 6206.
11 Z. Yang, M. She, J. Zhang, X. X. Chen, Y. Y. Huang, H. Y. Zhu, P. Liu, J. L. Li and Z. Shi, *Sens. Actuators, B*, 2013, **176**, 482.
12 H. Y. Lee, K. M. K. Swamy, J. Y. Jung, G. Kim and J. Yoon, *Sens. Actuators, B*, 2013, **182**, 530.
13 M. M. Yu, Z. X. Li, L. H. Wei, D. H. Wei and M. S. Tang, *Org. Lett.*, 2008, **10**, 5115.
14 H. S. Jung, P. S. Kwon, J. W. Lee, J. I. Kim, C. S. Hong, J. W. Kim, S. H. Yan, J. Y. Lee, J. H. Lee, T. Joo and J. S. Kim, *J. Am. Chem. Soc.*, 2009, **131**, 2008.
15 J. L. Yao, K. Zhang, H. J. Zhu, F. Ma, M. T. Sun, H. Yu, J. Sun and S. H. Wang, *Anal. Chem.*, 2013, **85**, 6461.
16 C. Kar, M. D. Adhikari, A. Ramesh and G. Das, *Inorg. Chem.*, 2013, **52**, 743.
17 J. H. Jang, S. Bhuniya, J. Kang, A. Yeom, K. S. Hong and J. S. Kim, *Org. Lett.*, 2013, **15**, 4702.
18 H. W. Engels, H. G. Pirkl, R. Albers, R. W. Albach, J. Krause, A. Hoffmann, H. Casselmann and J. Dormish, *Angew. Chem., Int. Ed.*, 2013, **52**, 9422.
19 H. Y. Yang, X. M. Zhang, L. J. Duan, M. Y. Zhang, G. H. Gao and H. X. Zhang, *J. Appl. Polym. Sci.*, 2013, 846.
20 J. L. Vilas, J. M. Laza, C. Rodríguez, M. Rodríguez and L. M. León, *Polym. Eng. Sci.*, 2013, 744.
21 T. Chen, W. P. Zhu, Y. F. Xu, S. Y. Zhang, X. J. Zhang and X. H. Qian, *Dalton Trans.*, 2010, **39**, 1316.